Proceedings of the ASME 2011 Pressure Vessels & Piping Division Conference
PVP2011
July 17-21, 2011, Baltimore, Maryland, USA

PVP2011-57960

A DIRECT-SEARCH COMPUTATIONAL WELD MECHANICS OPTIMIZATION USING LEAST-SQUARE APPROXIMATION

Mahyar Asadi *

Mechanical and Aerospace Engineering
Carleton University
Ottawa, Ontario, K1S 5B6
Canada
masadi@connect.carleton.ca

John A. Goldak

Mechanical and Aerospace Engineering
Carleton University
Ottawa, Ontario, K1S 5B6
Canada
jgoldak@mrco2.carleton.ca

ABSTRACT

Using a frame-work for exploring a design space in Computational Weld Mechanics (CWM), a recent direct-search algorithm from Kolda, Lewis and Torczon is modified to use a least-square approximation to improve the method of following a path to the minimum in the algorithm. To compare the original and modified algorithms, a CWM optimization problem on a 152 x 1220 x 12.5 mm bar of Aluminum 5052-H32 is solved to minimize the weld distortion mitigated by a side heating technique. The CWM optimization problem is to find the best point in the space of side heater design parameters: power, heated area, longitudinal and transverse distance from the weld such that the final distortion is as low as possible (minimized). This CWM optimization problem is constrained to keep the stress level generated by the side heaters, in the elastic region to avoid adding an additional permanent plastic strain to the bar. The number of iterations, size of DOE matrix required and CPU time to find the minimum for the two algorithms are compared.

INTRODUCTION

In general, optimization refers to finding/choosing the best element from some set of available alternatives. In other words, finding the best-available value(s) of some objective function f in a given domain [1]. This scalar function f depends on one or more independent variables and the goal is to find the value of those variables where f is a minimum [2].

Historically, most approaches to optimization use basically the Taylor's series expansion to a local-linearized approximations of the objective function. In fact, one can classify most methods for numerical optimization according to how many terms of the expansion are exploited [3]. Newton's method, for instance, is a second-order method based on the second-order Taylor polynomial approximation and therefore the first and second derivatives are required. Steepest descent, another instance, works with the first derivatives and local-linearized approximation based on the first-order Taylor polynomial. It is classified as a first-order method. In this taxonomy, zero-order methods rely exclusively on values of the objective function and do not require derivative information. They are direct-search methods, which indeed are often called zero-order/derivative-free methods in the engineering optimization community [3], [4].

There exist a great number of derivative-based optimization algorithms. The algorithms using the derivative are somewhat more powerful than those using only the values however they are limited in that the derivatives of both the objective function and the design parameters have to exist and if the objective function contains multiple extremum, then gradient converges to the nearest local extremum and will not find the global extremum.

However, there is no perfect algorithm for all forms of nonlinear optimization problems and it is strongly recommended that more than one algorithm be tried and compared [2]. For direct-search methods, Lewis, Torczon and Trosset in [3] advise that

*Address all correspondence to this author.

any practical optimizer includes direct-search methods among their many tools for optimization.

OBJECTIVE FUNCTION

Optimization problems start with one (or more) scalar objective function that determines how good a solution/result is. This scalar-valued function is basically defined by the user to characterize a favored behavior of a system. The specific form of such function comes from the nature of the problem and creativity of user. However, a p-norm could be a good function for many cases [5].

DIRECT-SEARCH ALGORITHM

Kolda, Lewis and Torczon have proposed a basic algorithm called "*Compass Search*" and an advanced one called "*GSS*" for direct-search optimization in [6]. Their ideas are summarized as a pseudo-code follow;

Given an objective function, a DOE-matrix framework and a starting point:
(A DOE-matrix framework is a set of design parameters with bounds on each parameter and a minimum step size and trial step size for each parameter)

1. Create a DOE matrix that respects the constraints.
2. Run DOE matrix and assess results;
3. If there is a new minimum with a sufficient decrease:
   Move to the minimum as a new trial point and go to 2.
4. If there is not a new minimum point:
   Test for convergence.
   If no convergence, refine the trial step size and go to 2.
   If convergence, write report and stop.

We employed this pseudo-code in our frame work and in the next section describe an improved method to follow the path to the minimum using least-square approximation.

LEAST-SQUARE ALGORITHM

Least squares methods, generally, approximate over-determined systems of equations such that the sum of the squares of the residuals becomes minimum. This method is the basis for the regression models that are frequently used to approximate the behavior of a system as a mathematical function of independent variables. We employed the least-square method to approximate the behavior of the objective function around our trial point and the regression coefficients, β, are calculated by Eq. 1 for $Y = X\beta$ where the $Y_{n\times 1}$ is the vector of n values of the objective function, $X_{n\times m}$ is the matrix of n sample points in design space and m terms in the regression model, $\beta_{m\times 1}$ computed from Eq. 1.

$$\beta = \left(X^T X\right)^{-1} X^T Y \tag{1}$$

The idea of using least-square approximation in direct-search optimization, is presented as the following pseudo-code:

Given an objective function, starting point, parameter's step-size and parameter's bounds construct a mesh or grid to discretize the design space

1. Create a DOE matrix that respects the constraints and run the DOE matrix (using MPI for example).
2. Assess results and construct the least-square regression model for the objective function (quadratic or higher).
3. Test for convergence.
   If converged, write report and stop.
4. If not, find values of parameters for the minimum of the regression equation.
5. If the minimum from regression approximation is smaller than accurate results in the DOE matrix then run the configuration of the regression-find minimum using the accurate model.
6. If the accurate model and the regression model agrees within a certain tolerance, move to the new configuration.
   If not, move to the minimum in the regression-tested region. Find the closest node on the mesh (or 2R-refined mesh) and perturb based on the gradient computed from the least-square approximation on the node picked.
7. Go to 2

Both algorithms: the original direct-search and the least-square direct-search, are employed in this paper to solve a CWM optimization problem to mitigate the distortion of an edge welded Aluminum bar using a side-heating technique. The CWM optimization problem is to find the point in the space of side heater design parameters that minimize the final distortion. The two algorithms are compared with respect to the number of iterations, size of DOE matrix required and CPU time to find the minimum in the discussion section.

EDGE-WELDED BAR SETUP

The test setup is an edge weld on a 152 x 1220 x 12.5 mm bar of Aluminium 5052-H32. The full computational model that includes transient thermal and stress analysis is analyzed by Vr-Weld software [7]. CWM validation is presented in [8] by comparison with an experimental data measured carefully by Masubuchi in [9].

The mesh employed is shown in Fig. 1 has 6600 8-node brick elements and 9680 nodes. The material was aluminum 5052-H32 alloy with chemical composition Al 96.7, Mg 2.5, Cr 0.25, Cu max 0.1, Fe max 0.4, Mn max 0.1, Si max 0.25, Zn max

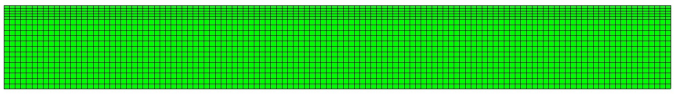

FIGURE 1. A 2D VIEW OF THE 3D MESH EMPLOYED IN THE ANALYSIS.

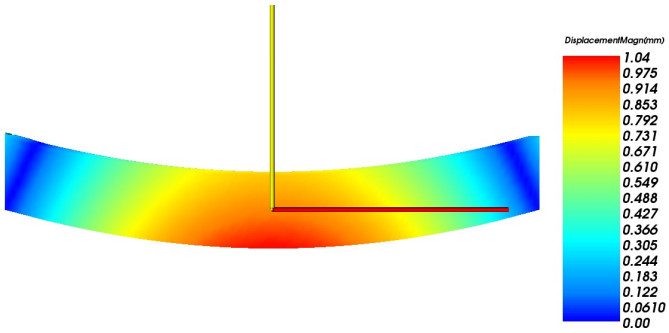

FIGURE 2. DEFLECTION IN Y DIRECTION AT THE END OF THE PROCESS (X85). RED AND YELLOW AXIS ARE X AND Y.

0.1 Wt %. The temperature dependent material properties of Al 5052-H32 were given in [9] and this data was employed in the analysis of this test. The gas metal-arc-welding process was employed to weld the specimen and the welding parameters were current 260 amperes, voltage 23 volts, travel speed 7.34 mm/s, filler metal Al-4043 with 1.6 mm wire diameter, wire feed speed 170 mm/s and the shielding gas was Argon. The specimen was allowed to cool to ambient temperature after welding was completed.

The stress analysis shows a significant Y-deflection illustrated in Fig. 2 and the goal is to mitigate this deflection in order to get as straight a bar as possible at the end of the process.

Okerblom [10] discussed different techniques for mitigation of distortion from welding. One of the techniques is to apply a transient thermal tension by side heaters [11]. This technique introduces a significant tension around the weld. The side heater's power, heated area, the distance from the weld either longitudinal or transversal are the design parameters for this technique.

The side heater source is characterized by a double ellipsoid model [12] moving parallel to the weld path. The power is computed from ηVI; side heater efficiency, current and voltage. Power is varied by changing η from 0.2 to 0.7 using fixed I and V equal to 260 amp and 23 V. Four semi-axes lengths of the parameters of the double ellipsoid geometry are assumed equal and therefore form a sphere. In effect, the area formed by the intersection of this sphere and the surface of the bar is the area that absorbs the power and therefore is one of the side heating parameters. We characterized this parameter, area, by a single value that is the radius of the sphere, R. This parameter ranges from 10 to 70 mm. The quasi-transient position of the side heater

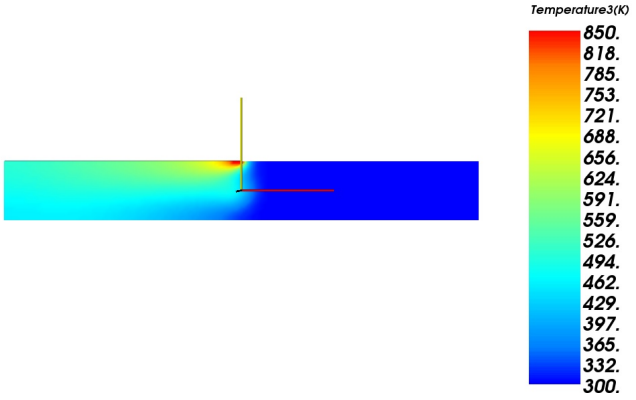

FIGURE 3. ORIGIN OF THE COORDINATE SYSTEM USED IN THE ANALYSIS. RED AND YELLOW AXIS ARE X AND Y.

wrt the weld, can be moved ahead/behind the arc or shifted closer or farther from the weld path. We put the origin of the coordinate system on the bar's centerline and exactly below the weld tip as shown in Fig. 3. The relative position of the side heater therefore can move in the X or Y direction. Finally, the side heater design parameters are; η, R, (X, Y), denote power, area's radius, longitudinal and transverse shift respectively.

The side heating could add plastic strain to the bar if the power density is too high. To avoid forming such plastic strain, power is constrained to be in the gray area in Fig. 4. This plot is drawn based on the plastic strain computed by FEM analyses when the side heater is applied with no weld. The gray area shows no-plastic-strain zone. Our analyses show that if the maximum temperature in the side heater stays below 480 $^{\circ}K$, the plastic strain does not form. Since thermal analysis requires much less CPU time than stress analysis, the upper limit of 480 $^{\circ}K$ can be used in a CWM optimization algorithm to apply this constraint.

COMPUTATIONAL MODEL

The full computational model that includes thermal and stress analysis are analyzed by VrWeld software [7]. The details of the model for transient thermal and stress analysis are described below.

Thermal Analysis

The 3D transient temperature is computed by solving the transient heat equation.

$$\dot{h} + \nabla \cdot (-\kappa \nabla T) = Q \tag{2}$$

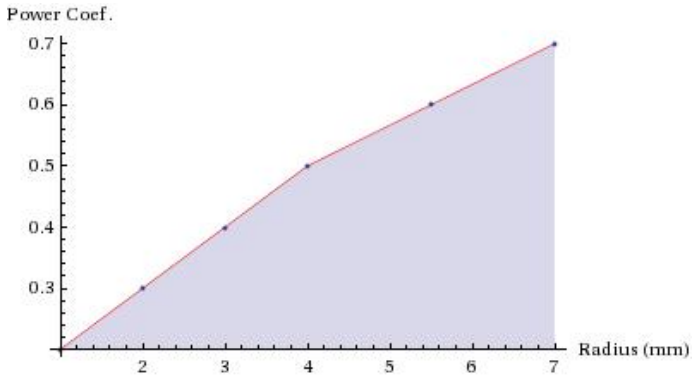

FIGURE 4. CONSTRAINT SHOWING THE FEASIBLE REGION FOR TWO SIDE HEATER PARAMETERS; POWER AND AREA. NODES ON THE GRAY ZONE HAVE THE MAXIMUM TEMPERATURE IN THE SIDE HEATER BELOW 480 $^{\circ}K$ AND THEREFORE GENERATE NO PLASTIC STRAIN.

where h is the specific enthalpy, the super imposed dot denotes the derivative wrt to time, κ is the thermal conductivity, T is the temperature, and Q is the power per unit volume or the power density distribution.

The transient heat equation was solved with a Lagrangian finite element method [13]. The initial temperature was 300 $^{\circ}K$. The power density distribution function Q $[w/m^3]$, the 'Double Ellipsoid' heat source model [12], was used with the heat source sizes; front, rear, width and depth set to 8, 16, 10 and 8 mm (see Fig 5).

A convection boundary condition generated a boundary flux q $[w/m^2]$ on all external surfaces. This flux is computed from Eq. 3 with ambient temperature of $T_{\text{ambient}} = 300^{\circ}K$ and convection coefficient as a function of temperature given in Eq. 4 extracted from [14] by interpolation of experimental data.

$$q = h_c(T - T_{\text{ambient}}) \tag{3}$$

$$h_c = 7.28 - \left(\frac{355000.0}{T^2}\right) + (0.001 \times T)\ [w/m^2K] \tag{4}$$

The time step length while welding was chosen so that in one time step the heat source was required to travel one element along the weld path. Filler metal was added as the welding arc moved along the weld path, i.e., the FEM domain changed in each time step during welding. After each weld pass was completed, the time step length was increased exponentially by a factor of 1.2 per time step until the the analysis was halted. The cool down time and the maximum temperature was 3600 seconds and 334 $^{\circ}K$ respectively when the analysis was halted.

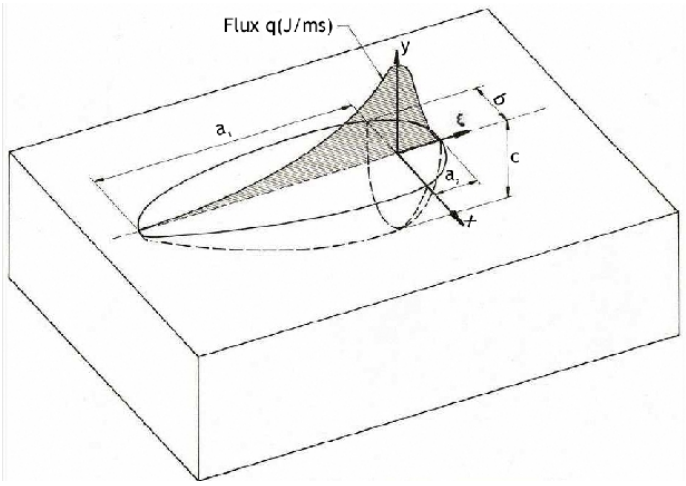

FIGURE 5. DOUBLE ELLIPSOID PARAMETERS; FRONT a_2, REAR a_1, WIDTH b, AND DEPTH c.

Stress Analysis

Given the density ρ, the elasticity tensor as a 6×6 matrix, the body force b and the Green-Lagrange strain ε, VrWeld solves the conservation of momentum equation that can be written in the form of Eq. 6 in which inertial forces, $\rho\,\ddot{x}$, are ignored.

$$\begin{aligned} \nabla \cdot \sigma + b &= 0 \\ \sigma &= D\varepsilon \\ \varepsilon &= (\nabla u + (\nabla u)^T + (\nabla u)^T \nabla u)/2 \end{aligned} \tag{5}$$

VrWeld solves this partial differential equation for a visco-thermo-elasto-plastic stress-strain relationship using theory and algorithms developed by J. C. Simo and his colleagues [15]. The initial state is assumed to be stress free. However, if the initial stress state was known, it could be initialized in VrWeld. The displacement boundary conditions for the test removed the rigid body modes by constraining the bottom left edge to zero displacement and to constrain the bottom right edge to zero transverse motion and zero vertical motion but allow horizontal translation.

The system is solved using a time marching scheme with time step lengths of approximately 3 seconds during welding and usually an exponentially increasing time step length when welding stops.

CWM OPTIMIZATION PROBLEM FOR THE EDGE-WELDED BAR

As a CWM optimization problem for the edge-welded bar, the objective is to obtain the values of η, R, X and Y such that the

TABLE 1. L_9 TAQUCHI DOE MATRIX EMPLOYED TO SCREEN THE OPTIMIZATION PARAMETERS WRT THE SENSITIVITY OF THE OBJECTIVE FUNCTION TO EACH PARAMETERS.

No.	R (m)	η	Y (m)	X (m)	Obj. Func.
1	40	0.3	-0.0162	-0.0508	0.099
2	40	0.4	0.0	0.0	0.090
3	40	0.5	0.0162	0.0508	0.148
4	50	0.3	0.0	50.8	0.134
5	50	0.4	0.0162	-0.0508	0.080
6	50	0.5	-0.0162	0.0	0.102
7	60	0.3	0.0162	0.0	0.091
8	60	0.4	-0.0162	0.0508	0.142
9	60	0.5	0.0	-0.0508	0.056

final distortion is minimized. Since the main deflection is in the normal direction to the weld (Y direction in our setup), the scalar objective function is picked as the L_1 norm of the final Y displacement along the bottom of the bar at the end of the process. If we set the position of nodes on undeformed geometry (original part before welding) to zero, the new position on deformed geometry (distorted part after welding) then can be defined as x in L_1 norm showing the nodal deformation. Total number of nodes in the L_1 norm calculation was 100 along the bottom of the bar. The next step in the multiple-design CWM optimization is to define an initial DOE matrix.

Taguchi [16] introduced several DOE matrices to explore the space of design parameters with a minimal number of tests and there are a great number of optimization efforts using his philosophy [17]. Although Taguchi's approach is an efficient method, a few concerns have been raised. Some of these concerns relate to the absence of higher-order interactions of design parameters. For these reasons, other approaches to carry out robust parameter design have been suggested including response modeling [18]. Since optimization algorithms require a start point and having a good start point leads to a better optimization, this suggested the optimization be started by a Taghuchi's DOE matrix to screen our parameters wrt the sensitivity of the objective function to each parameter. Therefore, an L_9 Taguchi DOE matrix was employed as given in Table 1 and the range of variations conforms with the constraint shown in Fig. 4.

The L_9 results show that the sensitivity of the objective function to the radius is high. This suggests minimizing the objective function, first, wrt to the radius separately. However the radius is linked to the power by the constraint (Fig. 4) and therefore we continue to minimize the objective function, wrt to the radius and power respecting the constraint. We picked a set of 4 nodes (0.04 m, 0.5),(0.04 m, 0.3),(0.02 m, 0.3),(0.03 m, 0.4) on the feasible region of the constraint and perturb Y and X with 3 levels around these nodes. This gives our second DOE matrix with 36 tests listed in Table 2. The reason for picking this set of nodes was that the tests number 10 and 27 were available from a previous stage and CPU time was saved by reading the result. However some other sets of nodes were tested and lead to the same conclusion.

The objective function values in Table 2 show that there is no interactions between parameters: (X, Y) and parameters: R, η because perturbation in (X, Y) gives the similar behavior for 4 settings of R and η in terms of sorting the objective function ascending/descending. In other words, (X, Y) perturbation has a pretty similar response surfaces shifted in different R, η. This DOE matrix indicates the optimum configuration of R and η is on a boundary line of the constraint toward the higher value of R and η. We reduced the upper bound of the radius to 6 cm to be narrower than the bar (7 cm) and therefore the optimum for the R and η is R = 6 cm and η = 0.6, i.e, 3588 J.

In order to find the optimum value of Y and X, both algorithms are implemented: a) the original direct-search algorithm, b) the least-square direct-search algorithm.

Original Direct-search algorithm

Given the objective function, a full factorial DOE matrix, the starting point of Y and X equal zero, the trial step size of 0.0162 m and 0.0508 m for Y and X and the minimum step size of 0.002 m and 0.003 m for Y and X, the algorithm generates the data and sequences in Table 3. This is illustrated graphically in Fig. 6 to show the path followed by the algorithm to the minimum.

Least-Square Direct-search algorithm

Given the objective function, a DOE-matrix framework, the starting point of Y and X equal zero, the trial step size of $\pm$ 0.02 m Y and X and the minimum step size of 0.002 m and 0.003 m for Y and X, The least-square direct-search algorithm results the data and sequences in Table 4 using least-square regression Eq. 6, 7 and 8. This is illustrated graphically in Fig. 7 to show the path followed by the least-square algorithm to the minimum.

$$Reg_1 = 8.65X^2 + 0.43X + 73.50Y^2 - 1.31Y^2 + 0.07 \quad (6)$$

$$Reg_2 = 11.45X^2 + 0.58X + 107.77Y^2 - 2.31Y^2 + 0.07 \quad (7)$$

$$Reg_3 = 14.59X^2 + 0.74X + 92.98Y^2 - 2.16Y^2 + 0.07 \quad (8)$$

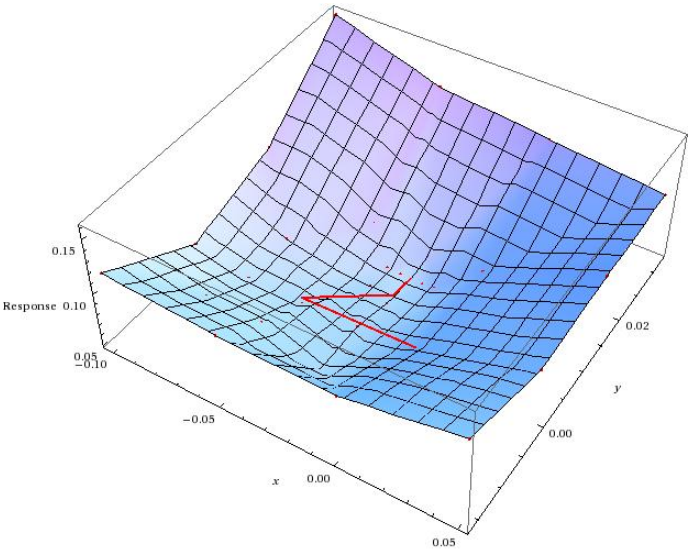

FIGURE 6. THE ORIGINAL DIRECT-SEARCH ALGORITHM RESULTS (TABLE 3) IS ILLUSTRATED GRAPHICALLY TO SHOW THE PATH FOLLOWED BY THE ALGORITHM TO THE MINIMUM.

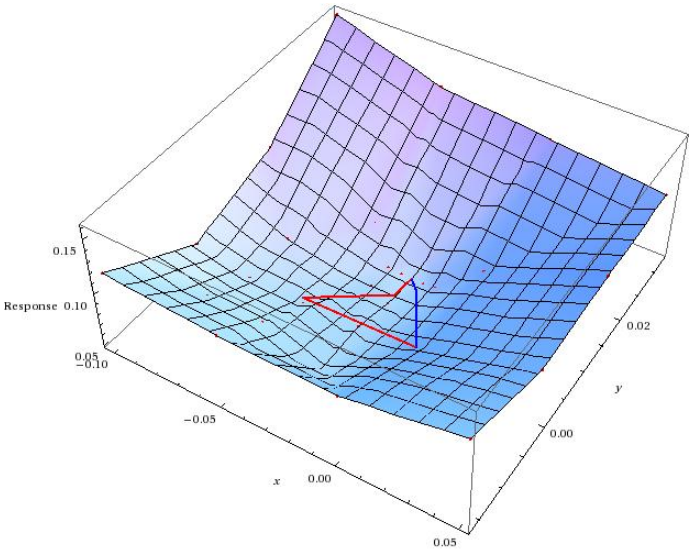

FIGURE 7. THE LEAST-SQUARE DIRECT-SEARCH ALGORITHM RESULTS (TABLE 4) IS ILLUSTRATED IN BLUE. IT IS COMPARED TO THE ORIGINAL DIRECT SEARCH IN RED (TABLE 3) TO SHOW THE PATH FOLLOWED BY EITHER ALGORITHMS TO THE MINIMUM.

COMPARISON AND DISCUSSION

Both algorithms find the same minimum, i.e., Y = -0.025 and X = 0.012 mm. The difference is the number of iterations required to find the minimum. The original direct-search algorithm does 6 iterations in comparison to the least-square direct-search with 3 iterations. Even the first iteration in the least-square algorithm gives a very close estimate to the minimum in contrast to the original direct-search algorithm in which the first iteration is far from the final results. In terms of CPU time, each thermal analysis took about 3 minutes and each stress analysis took about 45 minutes (total 48 minutes). The L_9 Taguchi DOE matrix has 9 tests run on 3 cores with total of 2 hours and 24 minutes. The η-and-R DOE matrix has 34 tests run on 4 cores with total of 7 hours and 12 minutes. Table 5 and 6 summarized the computation time and the number of cores used in each iteration for the original direct-search DOE matrix and the least-square direct-search DOE matrix respectively.

CWM RESULTS FOR THE OPTIMUM

The objective of the CWM optimization problem was to minimize the final deflection. Fig. 8 shows the final deflection for the weld with no side heater, with the side heater without weld and the weld with the side heater. Distance is from the left bottom corner to the right bottom corner of the bar and unit is meter.

Residual stress is usually interesting information for designers along with the information on deflection. Fig. 9 shows the longitudinal residual stress in the bar after welding is complete for the weld with no mitigation, when the side heater only is applied and the weld mitigated by the side heater. Residual stress is plotted for a line normal to the weld from the top edge to the bottom edge of the bar at the mid-length of the bar. Units are Pa and m for stress and distance respectively. The weld with side heater significantly reduces the residual stress in this cross-section.

It would be a simple matter to solve a DOE matrix to minimize longitudinal residual stress after welding was complete and the bar cooled to room temperature if one chooses an objective function. The question is what objective function to choose? Two possible choices are the maximum tensile residual stress or the integral of the square of the longitudinal stress over the cross-section $\int_0^W \sigma_{xx}^2 dW$ where W is the width of the bar. There are many other possible objective functions. Which norm is preferred would depend on the requirements the designer is trying to satisfy. It is also possible to have multiple objective functions and compute the Pareto optimal solutions.

CONCLUSION

A least-square direct-search method is presented in this paper to solve a constrained CWM optimization problem with a DOE matrix. Its performance is compared to an original direct-search algorithm. The CWM optimization problem is to minimize distortion of an edge-welded bar by using a side-heater technique with four design parameters. The optimal solution is

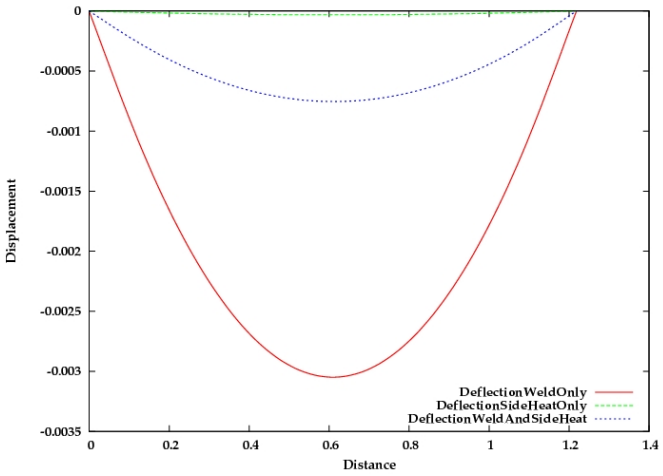

FIGURE 8. FINAL DEFLECTION FOR THE WELD WITH NO MITIGATION, WHEN THE SIDE HEATER ONLY APPLIED AND THE WELD MITIGATED BY THE SIDE HEATER. DISTANCE IS FROM THE LEFT BOTTOM CORNER TO THE RIGHT BOTTOM CORNER OF THE BAR AND UNIT IS METER.

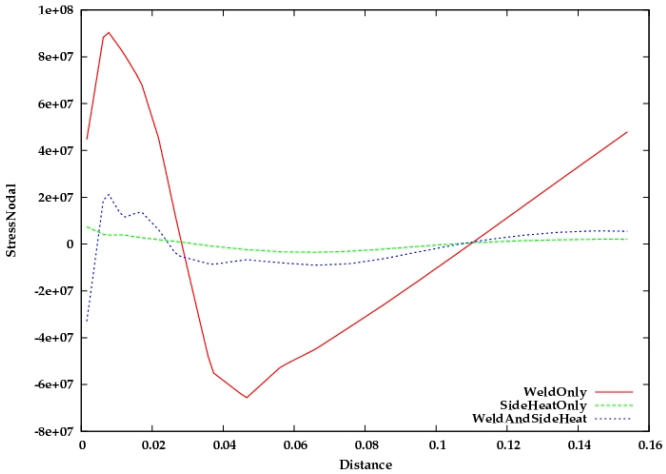

FIGURE 9. LONGITUDINAL RESIDUAL STRESS IN THE BAR AFTER WELDING IS COMPLETE FOR THE WELD WITH NO MITIGATION, WHEN THE SIDE HEATER IS ONLY APPLIED AND THE WELD MITIGATED BY THE SIDE HEATER. RESIDUAL STRESS IS PLOTTED FOR A LINE NORMAL TO THE WELD FROM THE TOP EDGE TO THE BOTTOM EDGE OF THE BAR AT THE MID-LENGTH OF THE BAR. UNITS ARE Pa AND m FOR STRESS AND DISTANCE RESPECTIVELY.

a heat source with 6 cm radius, power of 3588 J, located 2.5 cm behind the weld arc and 1 cm above the longitudinal center line of the bar minimizes the deflection. The deflection is plotted for the optimal design to show the improvement. In addition it is shown that minimizing the distortion, also reduces the longitudinal residual stress significantly. The method could be used to minimize the residual stress by solving a DOE matrix if one chooses an objective function.

Direct-search algorithms are more attractive with DOE matrix analyses that solve tens of computer models to explore or map the associated design space specified by a Design of Experiments (DOE) matrix to find optimal designs. In a multi-design frame-work, algorithms that use DOE matrices for more efficient searching are preferred. Such DOE matrix search takes advantage the fact that multiple trial solutions can be obtained simultaneously in contrast to sequential optimization that does search based on one-result at a time.

Coupling a least-square approximation in a regular direct-search algorithms followed the path to the minimum more efficiently in the neighborhood of a smooth basin. However the least-square approximation is not expected to work as well when the response surface is not a smooth basin, e.g., if the response surface is very wavy or rough. This is very similar to the expected behavior of a Newton-Raphson algorithm.

ACKNOWLEDGMENT

The authors wish to acknowledge Daniel Downy, Stainslav Tchernov and Jianguo Zhou from Goldak Technologies Inc. for their support. The authors are grateful to referees for their comments that led to improvements in this paper. The financial support of the National Science and Engineering Research Council (NSERC) is gratefully acknowledged.

TABLE 2. DOE MATRIX USED TO MINIMIZE THE OBJECTIVE FUNCTION WRT THE RADIUS AND POWER RESPECTING THE CONSTRAINT.

No.	R (m)	η	Y (m)	X (m)	Obj. Func.
1	0.03	0.4	0.0162	0.0508	0.112
2			0.0162	0.0	0.069
3			0.0162	-0.0508	0.071
4			0.0	0.0508	0.117
5			0.0	0.0	0.086
6			0.0	-0.0508	0.080
7			-0.0162	0.0508	0.145
8			-0.0162	0.0	0.127
9			-0.0162	-0.0508	0.129
10	40	0.5	0.0162	0.0508	0.099
11			0.0162	0.0	0.050
12			0.0162	-0.0508	0.057
13			0.0	0.0508	0.103
14			0.0	0.0	0.070
15			0.0	-0.0508	0.058
16			-0.0162	0.0508	0.135
17			-0.0162	0.0	0.114
18			-0.0162	-0.0508	0.115
19	40	0.3	0.0162	0.0508	0.137
20			0.0162	0.0	0.107
21			0.0162	-0.0508	0.111
22			0.0	0.0508	0.140
23			0.0	0.0	0.116
24			0.0	-0.0508	0.114
25			-0.0162	0.0508	0.160
26			-0.0162	0.0	0.146
27			-0.0162	-0.0508	0.148
28	20	0.3	0.0162	0.0508	0.129
29			0.0162	0.0	0.094
30			0.0162	-0.0508	0.093
31			0.0	508	0.134
32			0.0	0.0	0.108
33			0.0	-0.0508	0.106
34			-0.0162	0.0508	0.157
35			-0.0162	0.0	0.142
36			-0.0162	-0.0508	0.145

TABLE 3. DATA TABLE FOR THE ORIGINAL DIRECT-SEARCH ALGORITHM TESTED AND THE DECISION AT THE END OF EACH ITERATION. "C" INDICATES THE RESULT COPIED FROM PREVIOUS RUNS TO AVOID REPEATING THE ANALYSIS.

Iteration	Run No.	Y (m)	X (m)	Obj. Func.	Decision
1	1	0.0162	0.0508	0.1070	
	2	0.0162	0.0	0.0625	
	3	0.0162	- 0.0508	0.0642	
	4	0.0	0.0508	0.1012	
	5	0.0	0.0	0.0681	
	6	0.0	-0.0508	**0.0606**	
	7	-0.0162	0.0508	0.1299	
	8	-0.0162	0.0	0.1100	
	9	-0.0162	-0.0508	0.1113	Move
2	C	0.0162	0.0	0.0625	
	C	0.0162	-0.0508	0.0642	
	10	0.0162	-0.1016	0.0960	
	C	0.0	0.0	0.0681	
	C	0.0	-0.0508	**0.0606**	
	11	0.0	-0.1016	0.0703	
	C	-0.0162	0.0	0.1100	
	C	-0.0162	-0.0508	0.1113	
	13	-0.0162	-0.1016	0.1183	Refine
3	14	0.0081	-0.0254	**0.0512**	
	15	0.0081	-0.0508	0.0518	
	16	0.0081	-0.0762	0.0618	
	17	0.0	-0.0254	0.0623	
	C	0.0	-0.0508	0.0606	
	19	0.0	-0.0762	0.0602	
	20	-0.0081	-0.0254	0.0623	
	21	-0.0081	-0.0508	0.0820	
	22	-0.0081	-0.0762	0.0826	Move
4	23	0.0122	-0.0254	**0.0495**	
	24	0.0081	-0.0145	0.0526	
	C	0.0081	-0.0254	0.0512	
	26	0.0081	-0.0363	0.0514	
	27	0.0041	-0.0254	0.0554	Move
5	28	0.0162	-0.0254	0.0524	
	29	0.0122	-0.0145	0.0510	
	C	0.0122	-0.0254	**0.0495**	
	30	0.0122	-0.0363	0.0509	
	31	0.0081	-0.0254	0.0512	Refine
6	32	0.0145	-0.0254	0.0504	
	33	0.0122	-0.0200	0.0499	
	C	0.0122	-0.0254	**0.0495**	
	34	0.0122	-0.0309	0.0501	
	35	0.0101	-0.0254	0.0524	Stop

TABLE 4. DATA TABLE FOR THE LEAST-SQUARE DIRECT-SEARCH ALGORITHM TESTED AND THE DECISION AT THE END OF EACH ITERATION. "C" INDICATES THE RESULT COPIED FROM PREVIOUS RUNS TO AVOID REPEATING THE ANALYSIS.

Iteration	Run No.	Y (m)	X (m)	Obj. Func.	Decision
1	1	0.02	0.0	0.0714	Reg. Eq. 6
	2	0.0	0.02	0.0802	Y_{min} = -0.025
	3	0.0	0.0	0.0681	X_{min} = 0.009
	4	0.02	-0.02	0.0629	Reg. = 0.0569
	5	-0.02	0.0	0.1236	Acc. = 0.0508
					Move / Use 2R mesh
2	6	-0.02	0.02	0.0599	Reg. Eq. 7
	7	-0.01	0.01	0.0531	Y_{min} = -0.026
	8	-0.02	0.01	0.0506	X_{min} = 0.011
	9	-0.03	0.01	0.0505	Reg. = 0.0502
	C	-0.02	0.0	0.0629	Acc. = 0.0497
					Move / Use 4R mesh
3	10	-0.025	0.015	0.0510	Reg. Eq. 8
	C	-0.02	0.01	0.0506	Y_{min} = -0.025
	11	-0.025	0.01	0.0502	X_{min} = 0.012
	C	-0.03	0.01	0.0505	Reg. = 0.0502
	13	-0.025	0.005	0.0540	Acc. = 0.0495
					Converge / Stop

TABLE 5. CPU TIME FOR ALL CORES AND THE NUMBER OF CORES USED FOR EACH ITERATION IN THE ORIGINAL DIRECT-SEARCH DOE MATRIX.

Iteration	Num. of Cores	Num. of Analyses	CPU Time
1	3	9	2 h 24 m
2	3	3	48 m
3	4	8	1 h 36 m
4	4	4	48 m
5	4	4	48 m
6	4	4	48 m
		32	Total 7 h 12 m

TABLE 6. CPU TIME FOR ALL CORES AND THE NUMBER OF CORES USED FOR EACH ITERATION IN THE LEAST-SQUARE DIRECT-SEARCH DOE MATRIX.

Iteration	Num. of Cores	Num. of Analyses	CPU Time
1	3	5	1 h 36 m
Min test	1	1	48 m
2	4	4	48 m
Min test	1	1	48 m
3	3	3	48 m
Min test	1	1	48 m
		15	Total 5 h 36 m

REFERENCES

[1] The Free Encyclopedia, *http://en.wikipedia.org/wiki/Optimization–(mathematics)*, Accessed Jan 2011.

[2] W. H. Press, S. A. Teukolsky, W. T. Vetterling, B. P. Flannery, Numerical Recipes in C : The Art of Scientific Computing, Second edition, ISBN 0-521-43108-5, 1992.

[3] R. M. Lewis, V. Torczon, M. W. Trosset, Direct Search Method: Then and Now, J. Comput. Appl. Math., 124 (2000), pp 191-207, 2000.

[4] M. W. Trosset, I Know it When I See it: Toward a Denition of Direct Search Methods, SIAG/OPT Views-and-News: A Forum for the SIAM Activity Group on Optimization, 9 (1997), pp. 710, 1997.

[5] The Free Encyclopedia, *http://en.wikipedia.org/wiki/Lp-space*, Accessed Jan 2011.

[6] T. G. Kolda, R. M. Lewis, V. Torczon, Optimization by Direct Search: New Perspectives on Some Classical and Modern Methods, SIAM REVIEW, Vol. 45, No. 3, pp. 385482, DOI. 10.1137/S0036144502428893, 2003.

[7] Goldak Technologies Inc, *http://www.goldaktec.com/vrweld.html*, Accessed Feb 2011.

[8] M. Asadi, J. A. Goldak, Challenges in Verification of CWM Software to Compute Residual Stress and Distortion in Weld, Proceeding of the ASME 2010 Pressure Vessel and Piping Division Conference, Bellevue, Washington, PVP2010-25770, July 18-22, 2010.

[9] K. Masabuchi, Analysis of Welded Structures, MIT USA, Pergamon Press, International Series on Materials Science and Technology, Vol 33, Sec. 5 Transient Thermal Stress, pp.172 - 187, 1983.

[10] N. O. Okerblom, The Calculations of Deformations of Welded Metal Structures, Dept. of Scientific and Industrial Research, London, Translation from Russian, 1958.

[11] J. Song, J. Y. Shanghvi, P. Michaleris, Sensitivity Analysis and Optimization of Thermo-Elasto-Plastic Processes With Applications to Welding Side Heater Design, Computer Methods in Applied Mechanics and Engineering, 193, 4541-4566, DOI 10.1016/j.cma.2004.03.007, 2004.

[12] J. A. Goldak, A. Chakravarti, M. J. Bibby, A New Finite Element Model for Welding Heat Sources, Trans. AIME 186 Vol. 15B, pp. 299-305, June 1984.

[13] O. Zienkiewicz, R. Taylor, The Finite Element Method, Fourth Edition, Volume 2, McGraw-Hill, 1989.

[14] J. D. Francis, Welding Simulations of Aluminum Alloy Joints by Finite Element Analysis, M. Sc. Thesis Virginia Polytechnic Institute and State University, April 2002.

[15] J. C. Simo, Numerical Analysis of Classical Plasticity, Handbook for Numerical Analysis, Volume IV, ed. by P.G. Ciarlet and J.J. Lions, Elsevier, Amsterdam, 1998.

[16] G. Taguchi, Introduction to Quality Engineering , Asian Productivity Organization, Eighth Symposium on Taguchi Methods, American Supplier Institute, Dearborn, MI, USA, October 1990.

[17] R. Unal, E. B. Dean , Taguchi Approach to Design Optimization for Quality and Cost: An Overview, Annual Conference of the International Society of Parametric Analysts, 1991.

[18] ReliaSoft Corp. Online Course on DOE++ 2008, *http://www.weibull.com/DOEWeb/limitations-of-taguchis-approach.htm*, Accessed Sep 2010.